Journal of the Optical Society of Korea, Vol. 1, No. 1, March 1997, pp. 52~59

Parallel 3-dimensional optical interconnections using liquid crystal devices for B-ISDN electronic switching systems

Ho-In Jeon

Department of Electronic Engineering, Kyung Won University, Sung-Nam-Shi, 461-701, Korea

Doo Jin Cho

Department of Physics, Ajou University, Suwon 442-749, Korea

(Received; February 13, 1997)

In this paper, we propose a system design for a parallel 3-dimensional optical interconnection network utilizing variable grating mode liquid crystal devices (VGM LCD's) which are optical transducers capable of performing intensity-to-spatial-frequency conversion. The proposed system performs real-time, reconfigurable, but blocking and nonbroadcasting 3-dimensional optical interconnections. The operating principles of the 3-D optical interconnection network are described, and some of the fundamental limitations are addressed. The system presented in this paper can be directly used as a configuration of switching elements for the 2-D optical perfect-shuffle dynamic interconnection network, as well as for a B-ISDN photonic switching system.

I. INTRODUCTION

With the "information age" about to enter a new century, parallel distributed computing[1,2] and broadband communication networks are required to process and deliver a great amount of information. It is often realized that optics can take an important role in parallel processing and alleviate some of the communication bottlenecks, especially in the interconnection of high-speed systems. As the telecommunications and computer networks merge into one, many applications will rely on the advantages of optical interconnections and photonic switching.

Among the technologies that have been developed so far in the various parts of the world, integrated optics device technology has emerged as the most promising, owing to its rapid and numerous successes. Many components are now commercially available, ranging from optical modulators to polarization controllers, and to crossbar switches. For switching applications, arrays as large as 16×16 have been fabricated and field-tested, and problems such as polarization and wavelength sensitivity have been successfully resolved. Research is now moving from the $LiNbO_3$ substrate material to GaAs and InP for the obvious reason of facilitating the integration of guided wave optic components with electronics. This trend has resulted in research activities whose objective is the study and development of devices known as PICs (Photonic Integrated Circuits) and OEIC (Opto-Electronic Integrated Circuits) with higher integration density and increased functionality.

There are a number of reasons why guided wave optics has been regarded as the most promising technology in optical interconnections. One reason is that we can have flexible interconnects with low crosstalk and with no diffraction spreading due to propagation. The other is that the small transverse interaction areas and the selectable interaction lengths reduce the energy required to control the devices by orders of magnitude[3], and ensure compatibility with electron confinement volumes. Nevertheless, there are also drawbacks. Guided wave optics is a planar technology, and thus the inherent 3-D parallelism of optics is not utilized. In addition, the polarization sensitivity is in general aggravated in guided wave optics, since modal confinement factors and propagation constants are mode dependent[4].

Free-space grating optical interconnection systems have drawn a great deal of attention in the sense that they fully utilize the inherent 3-D parallelism of optics. The configuration in this architecture incorporates a medium in which the gratings are recorded. There are three possible types of gratings that may be used for this scheme. The first is the fixed holographic gratings recorded in photochemical materials such as dichromated gelatin and silver halide[5]. The second is the dynamic gratings that have been recorded in photorefractive materials such as $LiNbO_3$, $Bi_{13}SiO_{20}$, GaAs, and many more[6]. The last may be a spatial light modulator, exemplified by variable grating mode liquid crystal devices, that can change their gratings depending upon either the intensity of the incident beam

or the applied voltage controlled by external electronics.

The network design involves a trade-off between factors such as cost, ease of reconfiguration, contention (the possibility that messages may collide in certain network configurations), bandwidth, and control-complexity[7]. The crossbar interconnection network is known to be one of the most powerful interconnection networks in that it allows all processors and/or memories to be dynamically interconnected in an arbitrary permutation without contention and without moving any existing interconnections. The drawback of a crossbar is that its switching complexity grows as $O(N^2)$. Many different types of multistage networks with $O(N \log N)$ switches which provide parallel communications at a lower cost have been proposed[8]. However, these networks have limited permutation capabilities causing contention problems.

There have been several efforts to implement optical interconnection networks not only for VLSI systems[9], but also for optical processors[10]. Several researchers have suggested and implemented various optical interconnecting schemes. Several techniques are presented[11]; one is an optical digital computer configured as a parallel switching network, others are essentially optical methods of performing matrix-vector and matrix-matrix products. Several functional interconnection schemes using optical gates are described[12]. The implementation of both space-variant, space-invariant and hybrid interconnecting schemes using computer generated subholograms is given[10,13]. An optical implementation of the perfect shuffle exchange network using lenses and Wollaston prisms is presented[14]. A suggestion in optical crossbar networks using directional couplers is given[15], although it provides only a planar interconnection scheme which does not fully exploit the advantages of two-dimensional optical processing systems. A system design of 1-D optical crossbar interconnection network using variable grating mode liquid crystal devices has been introduced[16]. The design of 3-D optical interconnection networks using ferroelectric liquid crystals and 3-D dynamic optical interconnection network which performs 3-D omega network has been proposed in [17] and [18], respectively.

In this paper, we propose a system design for a 3-dimensional optical crossbar interconnection network utilizing variable grating mode (VGM) liquid crystal devices which are optical transducers capable of perforrming an intensity-to-spatial-frequency conversion. The proposed system performs a real-time, reconfigurable, but blocking, and nonbroadcasting 3-dimensional optical crossbar interconnections. In section 2, some properties of VGM devices are reviewed. Section 3 describes how the 3-D interconnection system works. The system analysis and its fundamental limitations are given in Section 4, and discussions on the proposed 3-D optical crossbar interconnection networks are addressed in the conclusion.

II. VGM LIQUID CRYSTAL DEVICES

Variable grating mode liquid crystal devices (VGM LCD) are a new class of optical transducers which can perform an intensity-to-spatial frequency conversion over a two dimensional image field. The VGM LCD primarily consists of a photoconductive layer in series with a layer of nematic liquid crystal mixture as shown in Fig. 1. When a dc bias voltage above a threshold is applied across the device to provide a voltage division between the two layers, a domain instability is formed in the liquid crystal layer as shown in Fig. 2. (The word "domain" in this paper is reserved for the description of the phenomenon of bright and dark stripes which appear when a dc voltage is applied across the device. This phenomenon, which is caused by the variation of the optical path length due to the periodic per-

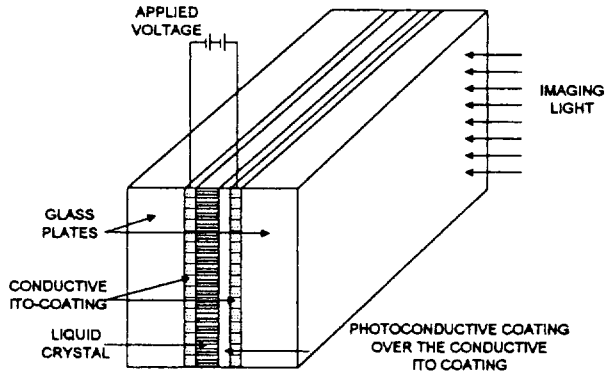

Fig. 1. Schematic diagram of the VGM device construction.

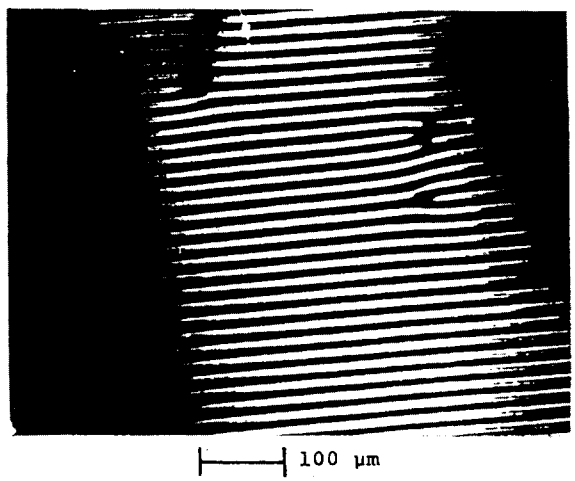

Fig. 2. Phase structure viewed through a polarizing microscope.

turbation of the liquid crystal uniaxial index ellipsoid, is generally named "domain structured instability" in liquid crystals). The width d of the domain period (line pair) is inversely proportional to the applied voltage V according to

$$d = \frac{\alpha}{V} \tag{1}$$

where α is a constant that is dependent on the particular liquid crystal.

When a write beam illuminates the cell, the input intensity causes the voltage across the photoconductive layer to decay and correspondingly enhances the voltage across the liquid crystal layer. It follows thus that the photoconductor implements an intensity-to-voltage conversion which changes the spatial frequency of the liquid crystal layer according to Eq. (1). The transverse conductivity of the photoconductor is generally low, so that the phase grating formed is highly local. If both processes are considered together, the device is seen to perform local intensity-to-spatial-frequency conversion. A collimated readout beam incident on the device at a wavelength where the photoconductor is insensitive is angle-encoded within each image pixel by diffraction from each induced phase grating and consequently can be steered in any one-dimensional direction orthogonal to the grating orientation.

When designing an optical interconnection system based on VGM devices, their operational properties must be considered. Some of these properties that we will consider in this section include: the accessible range of spatial frequencies, size of the diffraction orders, the functional dependence of diffraction efficiency on the applied voltage, maximum diffraction efficiency, response time, device uniformity, device input sensitivity, and the polarization characteristics of the device. Characteristics of these parameters can be found in [16].

The accessible range of spatial frequencies extends from the threshold for grating formation to the onset of dynamic scattering induced by high electric fields. The typical range of spatial frequencies is from 200 line pairs/mm to over 600 line pairs/mm. It has been reported that this accessible range can be extended by a factor of two by utilizing the orthogonal polarization behavior of alternating diffracted orders.

The size of the diffraction orders is determined by two factors: diffraction from finite-sized pixel apertures and grating imperfections that cause local deviations from constant spatial frequency. The most common type of grating imperfection is the joining or splitting of grating lines as shown in Fig. 2. This grating imperfection is not well understood, although it affects the performance of the optical interconnection systems. It is shown that, when a beam is incident on the imperfection, the spot size of the diffracted beam increases, which consequently increases unexpected crosstalk and thus reduces the maximum number of interconnection elements that can be obtained in one configuration of the interconnection. Some experimental results that have been made in Hughes Research Laboratory have shown that the degree of grating imperfection is proportional to the rate of change of applied voltage[19,20].

Unfortunately, the diffraction efficiencies of the VGM LCD have not been formulated analytically, nor have VGM LCD's been classified as one of thin or thick gratings. For simplicity of calculation, they are often regarded as thin gratings. The experimental results of the functional dependences of diffraction efficiency on the applied voltage have been considered in this paper to evaluate the overall diffraction efficiency of the system. As shown in Fig. 3, the diffraction efficiencies of the second order are higher than that of the first order and are approximately 20%. This phenomenon occurs due to the peculiar nature of the birefringent phase grating formed by the VGM distortion.

The slow response of the device is the major factor that inhibits the widespread utilization of VGM devices for optical interconnection systems. Work on measuring and improving the response time has been done at the Hughes Research Laboratory by Soffer *et al.*. The rise time for grating formation from below to above threshold is typically of the order one second, and the decay time is of the order 50 msec. The thickness effect on the VGM response time was also tested. It is seen in general that the thinner the cell, the shorter the

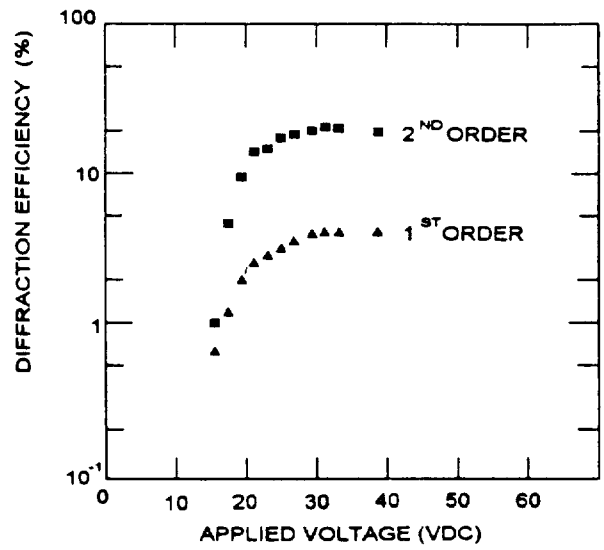

Fig. 3. Diffraction efficiency as a function of applied voltage across a nematic liquid crystal mixture of phenylbenzoate (HRL2N40).

turn-on time (delay time plus rise time). To improve the VGM response so as to be compatible with TV frame rates or faster, on the order of tens of milliseconds, Soffer *et. al.* have suggested a novel approach to, and some preliminary results for achieving a faster dynamic response by spoiling the long range order of the periodic domains. From the experiment, the rise time has been estimated to be 600±200 msec and the decay time to be only in the tens of milliseconds. Alternatives to the VGM device have also been studied in order to overcome the shortcomings—slow response and short degradation life-time. One alternative device that would preserve the essential feature (intensity-to-spatial frequency-conversion) would use electro-optically induced birefringent changes in a LC in wedge or prism-shaped devices. They have performed preliminary experiments to examine these ideas.

The input sensitivity of the VGM LCD, defined as the input (writing) intensity per unit area per unit change in grating spatial frequency, is determined by several factors. These include the slope of induced grating spatial frequency as a function of applied voltage for the particular nematic liquid crystal mixtures, the wavelength dependence of the photoconductive layer photoconductivity, and the cell switching ratio (fractional increase in voltage across the liquid crystal layer from illumination at the threshold for grating formation to saturation).

The uniformity of VGM LCD response depends on the layer thickness, on the homogeneous mixing of the liquid crystal material, and on the as-deposited spatial dependence of photoconductive sensitivity. Actually, the nonuniformity of the device response characteristics can be a contributing factor in the establishment of the maximum number of accessible gray levels and can be minimized significantly by improvements in the photoconductive layer deposition process.

III. OPERATING PRINCIPLES OF THE 3-D OPTICAL INTERCONNECTION NETWORK

In this section, a system which implements a real-time, reconfigurable, but blocking 3-dimensional optical interconnection network utilizing VGM LCDs, is presented. For the sake of clarity, we will briefly review the operating principles and some analyses of the one-dimensional VGM crossbar interconnection network that have been explained in detail in [16].

The one-dimensional VGM crossbar system is shown in Fig. 4. There are $2K+1$ electrical input lines, each driving a separate laser diode denoted by LD_i ($-K$, ..., i, ..., $+K$). The light from each laser diode separately illuminates one element in a 1-D array of $2K+1$ electrically controlled VGM cells (or subcells) as shown in Fig. 4. Any beam spreading or collimating optics is omitted for clarity. Each VGM cell of the 1-D array consists of a layer of nematic liquid crystal mixture placed between two transparent electrodes. There are no photoconductive layers in the structure. Thus the spatial frequency of a cell is controlled by the applied voltage. The Fourier transform lens forms the diffraction pattern of the VGM array in the back focal plane, where there is a mask to eliminate unwanted diffraction orders. A detector array in the back focal plane detects output signals from positive and negative diffraction orders and electrically combines them to produce an output in $2K+1$ parallel channels. Thus the VGM cells act as an electrically controllable beam steering array used to direct the input signal light to one of several spatially separated output channels.

It is shown [16] that the intensity distribution in the detector plane consists of $N = 2K+1$ sinc square functions which overlap each other in the Fourier transform plane. If the size of VGM cell is small, we can have many input channels, although large diffraction in the Fourier plane will cause crosstalk to adjacent output channels deteriorating the signal-to-noise ratio in the output plane. On the other hand, if the cell size is large, it reduces the maximum number of input channels because we have assumed that the overall dimensions of the array and the optical systems are fixed. Thus, there must be a trade-off between the maximum number of interconnection elements and the signal-to-noise ratio due to the crosstalk. The criterion for the trade-off was based on the fact that the signal-to-noise ratio in the output channel must be greater than 1 for the proper de-

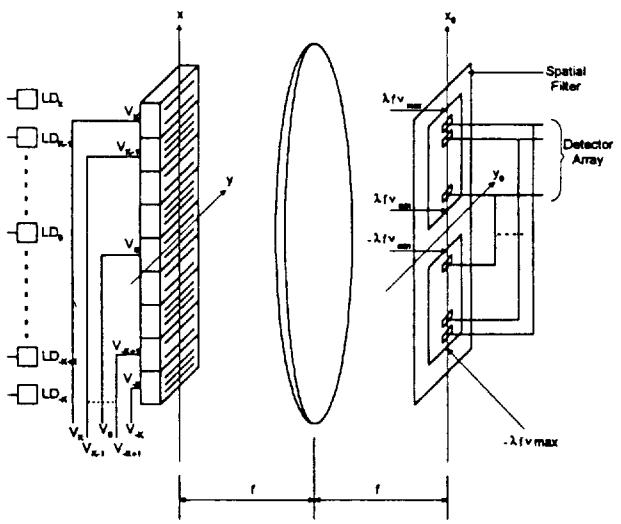

Fig. 4. Schematic Diagram of the 1-Dimensional optical crossbar interconnection network using VGM LCD.

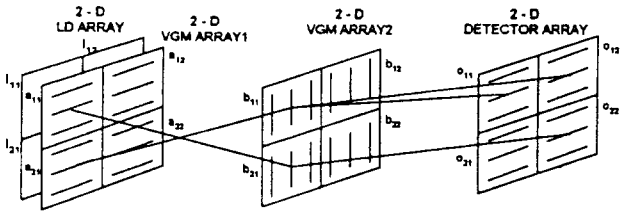

Fig. 5. Schematic diagram of the 3-Dimensional optical interconnections.

tection of signals in noise. A discussion of this problem and of other fundamental limitations such as reconfiguration time, diffraction efficiency, broadcasting, etc. is given in Sec. IV of reference [16].

The schematic diagram of a 3-D optical interconnection network is shown in Fig. 5. This is an extension of the 1-D VGM crossbar to 3-D optical interconnections. As described in the operating principles of 1-D VGM crossbar, the VGM cells can serve as an electrically controllable beam steering element array. The idea behind the extension is that it would be possible to implement a 3-D optical interconnection network by utilizing two arrays of VGM cells in cascade in such a way that the first array would be used for the vertical steering of input beams and the second for the horizontal steering. However, this scheme does not provide full N^4 interconnections because it causes a contention problem. This contention problem will be addressed in the following.

To explain the mechanism of interconnections between $N\times N$ input elements and $N\times N$ output elements, we designate each pixel of the two-dimensional input array by I_{ij} (i = 1, 2, ..., N, j = 1, 2, ..., N), that of VGM1 array by a_{ij}, that of VGM2 array by b_{ij}, and finally that of the two-dimensional output array by O_{ij}. Since VGM1 is placed in the proximity of the input plane, beams emanating from each pixel of the input are directly matched to the pixels of VGM1. In other words, an input beam I_{ij} is directed only by a_{ij}. For ease of manufacturing and operation, we assume that VGM1 is for vertical direction only, and VGM2 is for horizontal direction only. Therefore, I_{ij} can be connected to O_{ki} through a_{ij} and through b_{kj}. The simplest way of demonstrating this interconnection occurs will be the case when the input and output array is the size of 2×2 as shown in Fig. 5. All of the possible connections between 2×2 input and output arrays are shown in Table 1.

From the data shown in Table 1, we can see that all the elements in the input plane can be connected to any arbitrary element of the output plane with limited connectability. By "limited connectablility" we mean that, if one element of the input is connected the element of the output, another interconnection may not be obtained due to the blocking problem. To be more specific, suppose that I_{11} is to be connected to O_{11}. For this interconnection, a_{11} of VGM1 and b_{11} of VGM2 have to be involved. In this case, since b_{11} is already occupied, the only VGM cells that I_{21} can use is a_{21} followed by b_{21}, which consequently prohibit the connection to O_{12}. This is what we call the contention problem.

Table 1. Interconnections between input I_{ij} and output O_{kl} through 2-D VGM arrays a_{ij} and b_{kj}

I_{11}	a_{11}	b_{11}	O_{11}	I_{12}	a_{12}	b_{12}	O_{11}
I_{11}	a_{11}	b_{11}	O_{12}	I_{12}	a_{12}	b_{12}	O_{12}
I_{11}	a_{11}	b_{21}	O_{21}	I_{12}	a_{12}	b_{22}	O_{21}
I_{11}	a_{11}	b_{21}	O_{22}	I_{12}	a_{12}	b_{22}	O_{22}
I_{21}	a_{21}	b_{11}	O_{11}	I_{22}	a_{22}	b_{12}	O_{11}
I_{21}	a_{21}	b_{11}	O_{12}	I_{22}	a_{22}	b_{12}	O_{12}
I_{21}	a_{21}	b_{21}	O_{21}	I_{22}	a_{22}	b_{22}	O_{21}
I_{21}	a_{21}	b_{21}	O_{22}	I_{22}	a_{22}	b_{22}	O_{22}

Because of this contention problem, the number of maximum interconnection elements with the proposed system is limited by some factor as a function of N. Some parameters that determine the performance and the limitations of the proposed system will be presented in the next section.

IV. SYSTEM ANALYSIS

In this section, a performance analysis of the 3-D interconnection system and some fundamental limitations are given. These include the maximum number of interconnection elements that can be connected in one configuration, the reconfiguration time, and the overall diffraction efficiency.

The maximum number of interconnection elements that can be achieved in one configuration is one of the most important parameters that determine the efficiency of the system. For our analysis, we use two 2-D VGM arrays called VGM1 and VGM2, each of which has a dimension of 2×2 elements, for purposes of simplicity. As mentioned in Sec. 3, VGM1 is manufactured in such a way that all of the elements can direct input beams in a vertical direction, while VGM2 can do the same job in the horizontal direction. This is our basic assumption because liquid crystals do not form composite gratings, and once the domain instability is formulated, the single specific spatial frequency is dominated over all elements. Our objective is to connect all the 2×2 elements of the input plane to all the 2×2 elements of the output plane. To make sure that these 3-dimensional interconnections are made, we need a control scheme that has controllability of N^4 switches. Since we

are in the 3-dimensional space, this connection can never be achieved.

In order to generalize this blocking problem to the $N \times N$ input case, we first consider the cells located in the first column of the input plane. I_{11} can access, through a_{11}, any one of the first column of the VGM2 cells, and the number of these interconnections is N. One of the VGM2 cells that has been selected by I_{11} has N choices of pixels of the corresponding row of the output array, providing N^2 interconnections. At the same time, I_{21} can access any of the first column of VGM2 cells except the pixel that has been occupied by the I_{11} interconnection. This gives us (N-1) interconnections. One of the VGM2 cells that has been selected by I_{21} has N choices of pixels of the corresponding row of the output array, providing (N-1) · N interconnections. Continuing this process for the rest of the first column and combining all these interconnection numbers up to I_{N1}, we obtain the number of interconnections as

$$N \cdot N + (N-1) \cdot N + (N-2) \cdot N + \cdots + 1 \cdot N = \frac{N(N+1)}{2} N. \quad (2)$$

Now, consider the cells located in the second column of the input plane. I_{12} can access, through a_{12}, any one of the second column of the VGM2 cells, and the number of these interconnections is N. One of the VGM2 cells that has been selected by I_{12} at this time, however, has N-1 choices of pixels of the corresponding row of the output array, providing N · (N-1) interconnections. At the same time, I_{22} can access any of the second column of VGM2 cells except the pixel that has been occupied by the I_{12} interconnection. This gives us (N-1) interconnections. One of the VGM2 cells that has been selected by I_{21} has N-1 choices of pixels of the corresponding row of the output array, providing (N-1) · (N-1) interconnections. Continuing this process for the rest of the second column and combining all these interconnection numbers up to I_{N2}, we obtain

$$N \cdot (N-1) + (N-1) \cdot (N-1) + (N-2) \cdot (N-1) + \cdots + 1 \cdot (N-1) = \frac{N(N+1)}{2} (N-1). \quad (3)$$

Considering the rest of the columns of the input array, and rewriting the total number of interconnections, we obtain

$$N \cdot N + (N-1) N + \cdots + 1 \cdot N = \frac{N(N+1)}{2} N$$

$$N(N-1) + (N-1)(N-1) + \cdots + 1 \cdot (N-1) = \frac{N(N+1)}{2} (N-1)$$

$$N(N-2) + (N-1)(N-2) + \cdots + 1 \cdot (N-2) = \frac{N(N+1)}{2} (N-2)$$

$$N \cdot 1 + (N-1) 1 + \cdots + 1 \cdot 1 = \frac{N(N+1)}{2} 1$$

Summing up all the numbers of interconnections, we get the total of interconnections N_{total} as

$$N_{total} = \left[\frac{N(N+1)}{2} \right]^2. \quad (4)$$

Finally, by taking the square root on Eq. (4), we can compute the maximum number of interconnection elements that can be obtained in the input plane of the proposed system as

$$N_{max} = \sqrt{\left[\frac{N(N+1)}{2} \right]^2} = \frac{N(N+1)}{2} \quad (5)$$

We can check the validity of Eq. (5) by noting that, for the 2×2 input case, there are 9 interconnections giving 3 free choices of interconnection elements.

From this calculation, we can estimate the maximum number of interconnection elements that we can obtain using practical VGM devices. It is shown[16] that, if we let the size of the VGM device be 70×70 mm^2, and the maximum and minimum spatial frequency that can be formed in the device be ν_{max} = 400 cycles/mm, and ν_{min} = 800 cycles/mm, respectively, then 1-D VGM interconnection system can provide N = 127. Substituting this number into Eq. (5), we can get N = 8,128. This means that extension of 1-D VGM to 3-D interconnections gives us an increase in the number of maximum interconnection elements by a factor of (N + 1)/2 for the 1-D case.

If we define the interconnection efficiency η of the proposed system as the ratio of the total number of interconnections of the system to the number of interconnections for the 4-D crossbar case, we get

$$\eta = \frac{N_{max}}{N^2} = \frac{8128}{127 \times 127} = 50.39\% \quad (6)$$

It can be easily seen that, as the number of 2D cells increases, the utilization efficiency approaches asymptotically to 50%.

The reconfiguration time of the 3D interconnections based on VGM LCDs depends essentially on the response time of the VGM device used, since the response time of the VGM device reaches upto one second, which is a relatively long period of time compared with that required for driving the LD arrays. Thus, the reconfiguration time of the 3-D VGM in-

terconnection system can be estimated to be of the order of one second. However, this long reconfiguration time could be tolerated in applications where each connection is followed by the transfer of large blocks of data, such as in image processing. Taking into account attempts to improve the slow response of VGM by spoiling the long range order of periodic domains, and to find alternatives to the VGM devices which are being made at the Hughes Research Laboratory, shorter reconfiguration times should be available within a few years.

The overall diffraction efficiency of the system can be roughly calculated utilizing experimental results. Since the first order diffracted beam of the VGM's is used in this system, the diffraction efficiency of the system becomes $0.08 \times 0.08 = 0.0064 = 0.64\%$. However, if we insist on using the second order, it reaches upto $0.2 \times 0.2 = 0.04 = 4\%$. Although this low diffraction efficiency might discourage us from using the VGM LCDs as an optical interconnection network, it can be tolerated in some systems which do not require high diffraction efficiencies.

The non-broadcasting property of the VGM crossbar is one of the shortcomings discussed so far. This property can be explained by comparing the operating principles of VGM devices and those of acousto-optic cells. Acousto-optic devices have composite spatial frequencies of the phase grating according to the frequencies of applied electrical signal. On the other hand, The spatial frequencies of the phase grating formed in VGM devices are uniquely determined by the applied dc bias voltage. In other words, the phase grating is not of composite form but of a fundamental frequency. Thus, the VGM crossbar network cannot be used where broadcasting is required. However, since VGM crossbar is reconfigurable, smart algorithms for broadcasting could solve the problem.

V. DISCUSSIONS AND CONCLUSIONS

Advances in technology and the declining cost of computer hardware have encouraged us to design computer architectures consisting of a large number of processors executing programs concurrently. Such parallel computing architectures require communication networks between processors, and between processors and memories, which allow many processors to send data to other processors and/or memories simultaneously. Optical techniques for these communication purposes provide potential advantages, together with their inevitable disadvantages. Many results for implementing optical interconnection schemes have been reported in the literature. However, real-time, reconfigurable optical interconnection schemes have additional potential advantages for optical processors as well as broadband communication networks.

There are several ways to implement these. One of the possible schemes is to use two Acousto-optic Bragg cell arrays which can steer the input beam two-dimensionally. Another scheme is to use real-time holography and/or Computer Generated Holograms. Yet other schemes are utilizing Spatial Light Modulators. Techniques for implementing real-time optical interconnection networks utilizing directional couplers and matrix-vector and matrix-matrix processors have been reported.

In this paper, we have designed a real-time, reconfigurable, but blocking, and non-broadcasting 3-dimensional optical interconnection network exploiting the properties of VGM LCD's. The 4×4 3-dimensional optical interconnection network may be used for switching elements of the 3-D implementation of optical Omega network suggested by Sawchuk[15]. It is shown that extension of 1-D VGM to 3D interconnections gives us an increase in maximum interconnection elements by a factor of $(N+1)/2$ for the 1-D case. The overall diffraction efficiency of the system has been estimated to be 0.64%. However, if we use the second order of the VGM LCDs, we can obtain a diffraction efficiency of up to 4%. This low diffraction efficiency can be tolerated in some systems which do not require high diffraction efficiencies.

Acknowledgment

The present studies were supported in part by NON DIRECTED RESEARCH FUND, Korea Research Foundation, 1993, and in part by the Basic Science Research Institute Program, Ministry of Education, 1996, Project No. BSRI 96-2415.

REFERENCE

[1] Kai Hwang, F. A. Briggs, *Computer Architecture and Parallel Processing*, New York, McGraw-Hill, 1984.

[2] M. J. Flynn, "Some Computer Organizations and Their Effectiveness," *IEEE Trans. Computers*, Vol. C-21, No. 9, pp. 948-960, September 1972.

[3] T. Tamir, *Guided Wave Optoelectronics*, 2nd Edition (T. Tamir, Ed.), Springer-Verlag, Berlin, 1985.

[4] Lars Thylen, "$LiNbO_3$ and Semiconductor Guided Wave Optics in Switching and Interconnects," in *Photonic Switching and Interconnects*, 1st Edition (A. Marrakchi, Ed.), pp. 1-76, Marcel Dekker Inc., New York, New York, 1994.

[5] R. J. Collier, C. B. Burckhardt, and L. H. Lin, *Optical Holography*, Academic Press, Orlando, Fl., 1971.

[6] P. Gunter and J. P. Huignard (eds.), *Photorefractive Materials and Their Applications, I, II,* Topics in Applied Physics, Springer-Verlag, Berlin and Heidelberg, 1988.

[7] T. Y. Feng, "A Survey of Interconnection Networks," *IEEE Computer,* pp. 12-27, December 1981.

[8] C. L. Wu, T. Y. Feng, "On a Class of Multistage Interconnection Networks," *IEEE Trans. Computers,* Vol. C-29, pp. 694-702, August 1980.

[9] J. W. Goodman, "Optical Interconnections for VLSI Systems," *Proc. IEEE,* Vol. 72, pp. 850-866, July 1984.

[10] B. K. Jenkins, A. A. Sawchuk, and T. C. Strand, "Architectures for a Sequential Optical Logic Processor," *Proc. of the 10th IOCC,* pp. 6-12, April 1983.

[11] A. A. Sawchuk, B. K. Jenkins, C. S. Raghavendra, and A. Varma, "Optical Interconnection Networks," *Proc. Int. Conf. on Parallel Processing,* St. Charles, Ill, pp. 20-23 1985.

[12] A. Huang, "Architectural Considerations involved in the Design of an Optical Digital Computer," *Proc. IEEE,* Vol. 72, pp 780-786, July 1984.

[13] B. K. Jenkins, T. C. Strand, "Computer Generated Holograms for Space-Variant Interconnections in Optical Logic Systems," *Int. Conf. on Computer Generated Holography,* ed. by S.H. Lee, Proc. SPIE 437, pp. 110, 1983.

[14] A. Lohmann *et al.*, "Optical Implementation of the Perfect Shuffle," *Optical Computing Conference,* OSA, WA 3-1, March 18, 1985.

[15] H.S. Hinton, "A Nonblocking Optical Interconnection Network Using Directional Couplers," *Proc. IEEE Global Telecommunication Conference,* Atlanta Georgia, IEEE Catalog No. 84CH2064-4, pp. 885-889, November 1984.

[16] Ho-In Jeon and A. A. Sawchuk, "Optical Crossbar Interconnections Using Variable Grating Mode Devices," *Applied Optics,* Vol. 26, No. 2, pp. 261-269, January 15, 1987.

[17] Joe Shamir and Kristina M. Johnson, "The Design of Three-Dimensional Optical Interconnection Networks Using Ferroelectric Liquid Crystals," *Proceedings of 14th Congress of the Internationa Commission for Optics, Proceedings of the SPIE,* Vol. 813, pp. 541-542, August 24-28, 1987.

[18] Alexander A. Sawchuk, "3-D Optical Interconnection Networks," *Proceedings of the 14th Congress of the International Commission for Optics, Proceedings of the SPIE,* Vol. 813, pp. 547-548, August 24-28, 1987.

[19] B. H. Soffer *et. al.*, "Optical Computing with Variable Gratimg Mode Liquid Crystal Devices," *Proc. SPIE,* Vol. 232, 128, 1980.

[20] B. H. Soffer, "Real-Time Implementation of Nonlinear Optical Processing Functions," *Final Technical Report of Contract F49620-81-C-0086, Hughes Research Laboratories,* Malibu, CA. (15 June 1981-15 June 1984).